

# A Low Noise and High Sensitivity Image Sensor with Imaging and Phase-Difference Detection AF in All Pixels

M.Kobayashi, M.Johnson, Y.Wada, H.Tsuboi, T.Ono, H.Takada, K.Togo,  
T.Kishi, H.Takahashi, T.Ichikawa, S.Inoue

Canon Inc., 70-1, Yanagi-cho, Saiwai-ku, Kawasaki-shi, Kanagawa 212-8602, Japan

Phone: +81-3-3758-2111, Fax: +81-44-520-3218

E-mail: kobayashi.masahiro@canon.co.jp

## Abstract

In this paper, we describe a device structure and optical design for a CMOS image sensor with the phase-difference detection photodiodes (PD) for an autofocus (AF) function. This image sensor has a pixel separated into two PDs by a PN junction. All the effective pixels function as both the imaging and the phase-difference detection AF (PDAF). We have realized a low dark random noise ( $=1.8e^-$  at 1PD,  $2.5e^-$  at 1pixel) and high sensitivity ( $=78,000e^-/lx \cdot sec$  at 1green pixel) image sensor with the imaging and the PDAF functions in all the effective pixels.

## Introduction

Recently, image sensors with the PDAF function at image plane has been developed [1], [2]. These realize the AF function by arranging exclusive pixels to detect the phase-difference. In these image sensors, a pair of partially light shielded PD is arranged in a part of pixel array. The focusing speed is extremely fast in comparison with conventional contrast detection AF. The sensitivity, however, is degraded by the light shielding structure and interpolation processing by neighboring pixels is necessary for image generation [2]. Therefore, the number of pixels for AF function is limited to avoid the deterioration of image quality.

In this work, we developed an image sensor with the imaging and the PDAF functions in all the effective pixels without exclusive pixel for AF function. All the effective pixels have two PDs each

to detect phase-difference in one pixel without partially light shielding structure. Therefore, one pixel works as one AF point, and the sum of two PD outputs equals one pixel output.

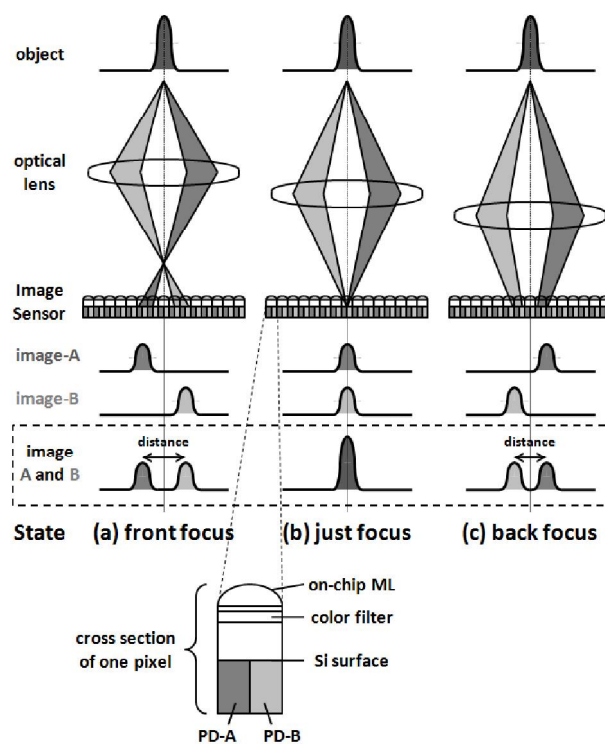


Fig. 1: Principle of the PDAF function

## Principle

Fig. 1 shows the principle of the PDAF function. Exit pupil of an optical lens and a PD of the image sensor are in optically conjugate relation by on-chip micro-lens (ML). Therefore, each pixel by separating into two PDs has the pupil split function for the PDAF function. A light flux which passes through a right half of the optical lens is led to the PD-A (the

PD at left side) and which passes through a left half of the optical lens is led to the PD-B (the PD at right side).

Defocusing amount is calculated from distance between the peak of the image-A (the image provided from PD-A group) and the peak of the image-B (the image provided from PD-B group).

The direction of the peak shift of the image-A and image-B is opposite between the front focus state and the back focus state.

These mean that in the camera system the optical lens is driven to a just focus instantly by calculated defocusing amount and the direction [3].

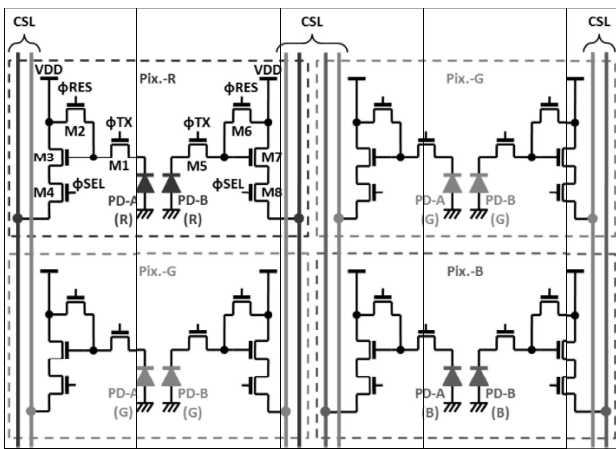


Fig. 2: Schematic view of 2x2 pixels

### Pixel Architecture

Fig. 2 shows the schematic view of 2x2 pixels. One pixel consists of two sub-pixels, and has one on-chip ML and one color-filter (CF) each. One sub-pixel consists of one PD, one floating diffusion (FD), four transistors for one signal output and one column signal line (CSL), thus one pixel consists of two PDs, eight transistors and two CSLs. A pair of sub-pixel is symmetrically arranged left and right. To achieve 60frames per second readout speed, four CSLs are driven simultaneously.

Fig. 3 shows the cross section diagram of the pixel. The PD-A and the PD-B are separated by a PN junction. The PN junction separation does not consist of the insulating materials (e.g. SiO<sub>2</sub>). By using the PN junction separation, non-sensitive area is minimized, light reflection at Si/SiO<sub>2</sub> boundary is reduced and defects at Si/SiO<sub>2</sub>

interface is decreased. It is reported that band-gap shrinkage at Si/SiO<sub>2</sub> interface causes dark current and defects increase [4], [5].

In addition, an impurity concentration of the p-type region for the PN junction separation is lower than that of the surface region forming the pinned PD. Therefore, recombination rate in the p-type impurity separation region is low, and the loss of the incident light is minimized. The incident light is divided into PD-A and PD-B, as a result, low noise and high sensitivity image sensor is realized.

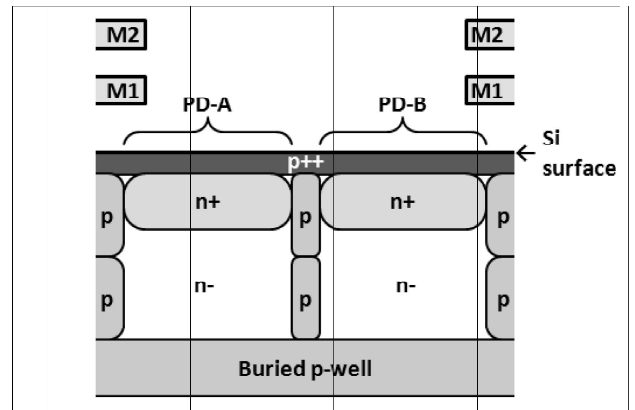


Fig. 3: Cross section diagram of the pixel

### Optical Design

We performed a three-dimensional finite difference time domain (FDTD) optical simulation and a transient analysis device simulation to determine the curvature of the on-chip ML.

Fig.4 shows the simulated ML curvature dependence of the light intensity profiles for perpendicular green incident light ( $\lambda=550\text{nm}$ ) to the image sensor surface, superimposed on the image sensor structure diagram. A dark color means that the light intensity is strong. The condensing position of the incident light changes depending on the ML curvature.

The figure also shows the incident light angle dependence of the quantum efficiencies (QE) of PD-A, PD-B and the sum of the two PDs. In the case (b) (the radius of curvature (RC) is  $4.3\mu\text{m}$ ), the simulated QE of a two PDs summation is 59.5%, higher than the case (a) (RC= $3.3\mu\text{m}$ ) 51.6% and the case (c) (RC= $5.3\mu\text{m}$ ) 55.1%. By adding signals of two separated PDs, the sensitivity is equivalent to that

of one PD structure.

The bottommost figure shows the incident light angle dependence of the QE ratio of PD-A to PD-B in the positive angle region and ratio of PD-B to PD-A in the negative angle region. The angle range below the ratio of 0.2 is compared in three cases. In the case (b), the angle range is 25 degrees. The range is wider than the case (a) 21 degrees and the case (c) 24 degrees. That wider range means the image-A and the image-B can separate at wider range of the incident light angle, and the AF performance is improved. Similarly, the angle range

above the ratio of 0.2 near 0 degrees is compared. In the case (b), the angle range is 9 degrees. The range is narrower than the case of (a) 10 degrees and the case of (c) 15 degrees. The narrower range near 0 degrees means the separation of image-A and the image-B is better at larger F-number (=smaller aperture). To realize both high sensitivity and high AF performance in the design of two PDs and one ML with the PDAF function, the accurate simulation of the height, the curvature and the shape of the ML is required.

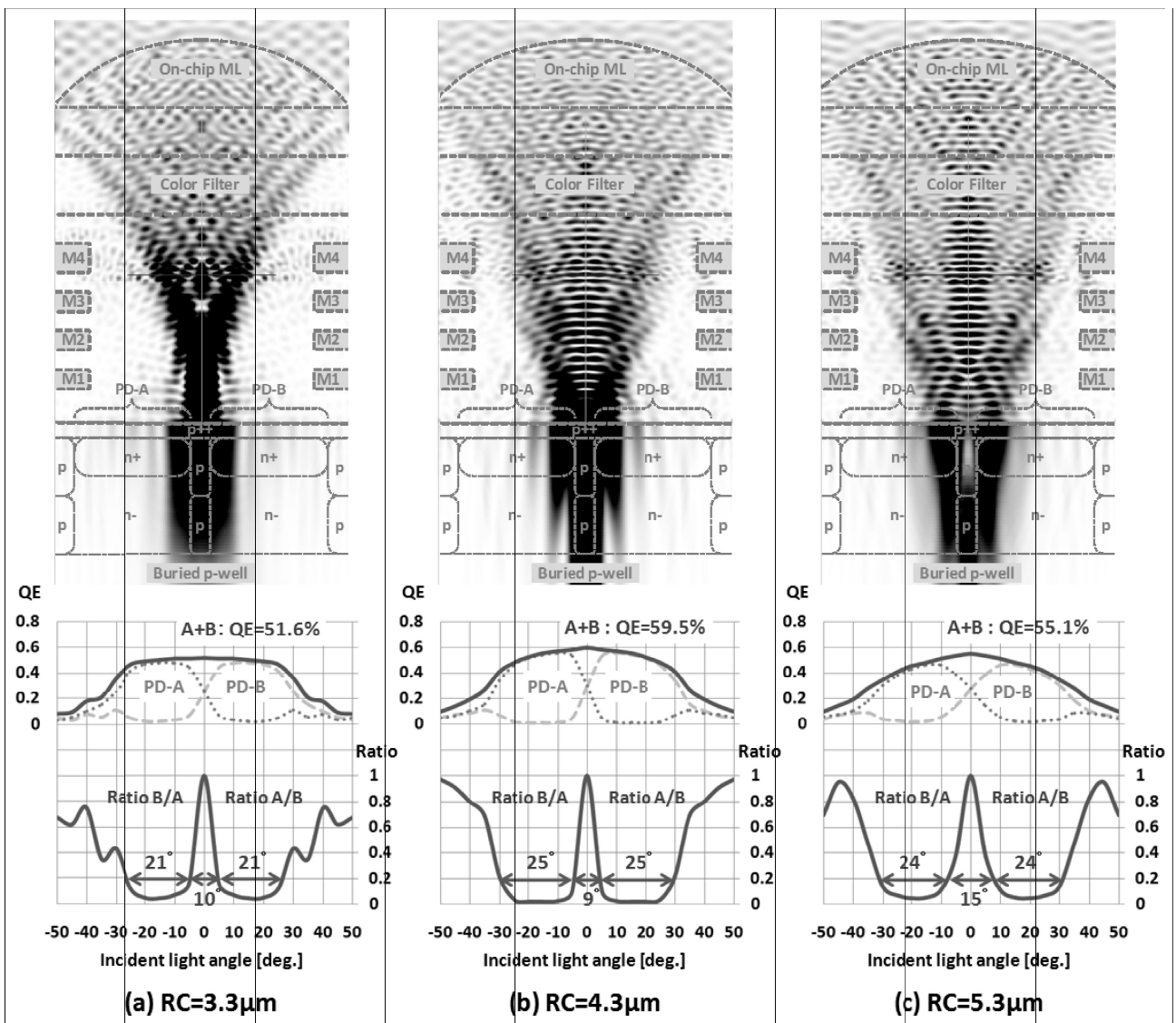


Fig. 4: Simulated ML curvature dependence of the light intensity profiles, Incident light angle dependence of the QE and the ratio of PD-A and PD-B

## Summary

Table 1 summarizes the specifications and the performances of this image sensor. Fabrication process is 0.18 $\mu\text{m}$  1Poly 4Metal CMOS process. Optical format is super 35mm. Pixel size is 6.4  $\mu\text{m}$  x 6.4  $\mu\text{m}$ . Number of effective pixels and the PDAF points are both 9.2M. Number of effective PDs is 18.5M. Full well capacity is 40,000e<sup>-</sup> (@one pixel = two PDs). Sensitivity is 78,000e<sup>-</sup>/lx\*s (@2,856K light source with IR-cut-filter; one green pixel). Dark random noise is 1.8e<sup>-</sup> at one PD and 2.5e<sup>-</sup> at one pixel (@gain=32, RT). Dark current is 50e<sup>-</sup> at one pixel (@60°C, one second). Maximum frame rate is 60frames per second with full pixel readout.

Fig. 5 shows the package photograph of this image sensor. Chip size is 29.9mm x 21.6mm.

High grade and high speed imaging has been achieved by the low noise and high sensitivity image sensor with imaging and phase-difference detection AF in all pixels.

## Acknowledgement

The authors would like to thank K.Kawabata, T.Kato, J.Iwata, Y.Arishima, A.Okita, A.Takabayashi, I.Onuki and Y.Harada the member of Canon Inc. for their contribution to this work.

Table 1: Summarized specifications and performances of this image sensor

Process	0.18 $\mu\text{m}$ 1P4M CMOS
Chip size	29.9 mm(H) x 21.6 mm(V)
Power supply	3.3V (Analog), 1.8V (Digital)
Maximum full frame rate	60 fps
Optical format	Super 35mm
Pixel size	6.4 $\mu\text{m}$ x 6.4 $\mu\text{m}$
Pixel architecture	2PD, 8Tr. each
Number of total pixels	4206(H) x 2340(V)
Number of effective pixels (=Auto-Focus points)	4112(H) x 2248(V) =9.2M
Number of effective photodiodes	8224(H) x 2248(V) =18.5M
Conversion gain	70 $\mu\text{V}/\text{e}^-$
Sensitivity @ 1pixel(=2PDs)	78000 e <sup>-</sup> /lx*s
Full well capacity @ 1pixel	40000 e <sup>-</sup>
Dark Random Noise @ gain=32, RT	1.8 e <sup>-</sup> rms (1PD), 2.5 e <sup>-</sup> rms (1pixel)
Dark Current @ 60°C, 1sec., 1pixel	50 e <sup>-</sup>

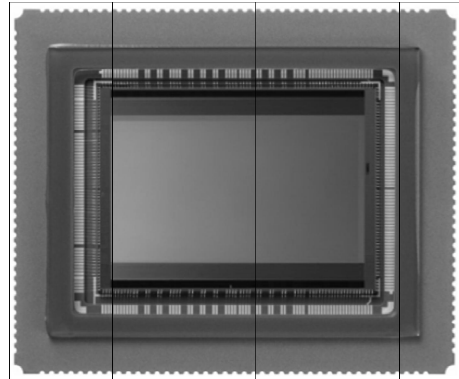


Fig. 5: Package photograph of this image sensor

## References

- [1] S.Uchiyama, "Superiority of Image Plane Phase Detection AF", ITE Technical Report, 36.38 (2012): 17.
- [2] H.Endo, "Phase Detection Pixel Built-in Image Sensor" to Realize High Speed Auto Focus", The journal of the Institute of Image Information and Television Engineers, 65.3 (2011): 290-292.
- [3] I.Onuki, "Digital Camera with Phase Detection Image Sensor", The journal of the Institute of Image Information and Television Engineers, 68.3 (2014): 203-207.
- [4] K.Takeuchi, et al., "Si band-gap shrinkage caused by local strain at Si/SiO<sub>2</sub> edge", Applied physics letters, 61.21, (1992): 2566-2568.
- [5] K. Itonaga, et al., "Extremely-Low-Noise CMOS Image Sensor with High Saturation Capacity", Electron Devices Meeting (IEDM), 2011 IEEE International. IEEE, 2011.